Extended Abstracts of the 2005 International Conference on Solid State Devices and Materials, Kobe, 2005, pp.62-63

C-2-2

Microstructural evolution of MIM capacitor prepared by ALD system at elevated temperature

C. H. Lin[1], C. C. Wang[1], P. J. Tzeng[1], C. S. Liang[1], W. M. Lo[1], H. Y. Li[1], L. S. Lee[1], S. C. Lo[2], Y. W. Chou[2], and M-J Tsai[1]

[1]Electronics Research and Service Organization
[2]Material Research Laboratory
Industrial Technology Research Institute
Chutung, Hsinchu 310, Taiwan
Phone : 886-3-5917148, Fax : 886-3-5917690
E-mail : linchahsin@itri.org.tw

1. Abstract

The raised-hollow holes were observed in the $TiN/Al_2O_3/HfO_2/Al_2O_3/TiN/SiO_2/Si$ multi-stack MIM (metal-insulator-metal) capacitor sample after 1000°C, 60 seconds rapid thermal annealing (RTA) process in N_2. At this high temperature, the TiN and Al_2O_3 were intermixed and partially re-crystallized. Also, the EDS (Energy Dispersive Spectroscopy) results indicated that the nitrogen in TiN was desorbed and the TiN was phase transformed to TiO_2. This phenomenon might result from the intermixture of TiN and Al_2O_3 and re-oxidation process during the high-temperature thermal annealing.

2. Introduction

The MIM capacitor with high-k dielectric layer is the mainstream of the DRAM storage node at 80 nm technology node and beyond [1]. However, for trench-structure capacitor, the higher thermal budget during the transistor fabrication can result in the degradation of high-k dielectric layer since the temperature may rise to around 900 °C during the source/drain activation step [2]. Hence, it is necessary to further verify the endurance of MIM capacitor with much higher thermal budget (in this study, 1000 °C is employed) to assure the reliability.

The TiN is a major candidate of the electrode of the MIM capacitor because the superior step coverage capability when deposited with an ALD system [3]. Hence, in this study, we investigated the microstructural evolution of $TiN/Al_2O_3/HfO_2/Al_2O_3/TiN/SiO_2/Si$ MIM capacitor sample with TiN electrode after 1000°C RTA.

3. Experimental results and discussions

Figures 1 and 2 show the Atomic force microscopy (AFM) topography and Scanning Electron Microscopy (SEM) morphology of MIM sample before and after RTA individually. As seen in Fig. 1, the sample with 1000 °C RTA had a much rougher surface. For the SEM pictures (Fig. 2), some irregular and raised spots were observed on the surface of annealed sample. This phenomenon resulted from the destruction of multi-stack structure. To further investigate this phenomenon, FETEM (Field Emission Transmission Electron Microscopy) and EELS (Electron Energy Loss Spectroscopy) were employed to analyze the samples.

Figure 3 shows the TEM micrograph of $TiN/Al_2O_3/HfO_2/Al_2O_3/TiN/SiO_2/Si$ multi-stack MIM sample. A raised-hollow hole can be observed obviously. Figure 4 shows the EELS spectra at various locations which are identified in Fig. 3. Figure 5 shows the Ti-O bonding signal extracted from the curve (1) of the Fig. 4 (location 1 of the Fig. 3). The hollow hole (location 7 of the Fig. 3) can be evidenced by the EELS data since no signal was observed. Also, the Ti-O bonding can be clearly seen in the locations 1 and 3 (Fig. 3). This indicated that the top and bottom TiN were fully oxidized and became TiO_2 since none of the N bonding signal (around 400 eV) was observed.

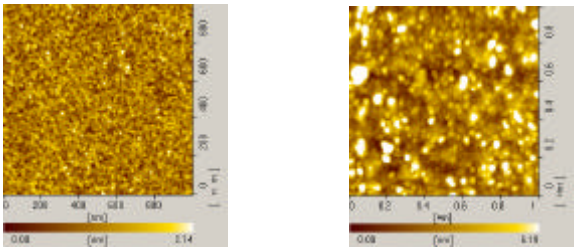

Before RTA (Ra=0.263nm) After RTA (Ra=1.148nm)

Fig. 1 AFM topography of MIM samples before and after RTA.

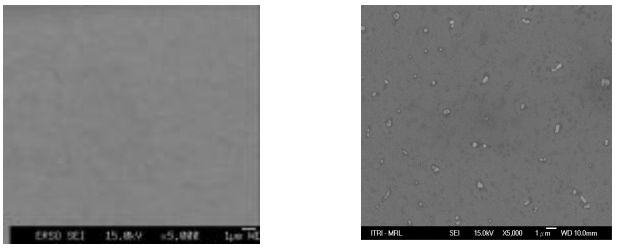

Before RTA After RTA

Fig. 2 SEM morphology of MIM samples before and after RTA.

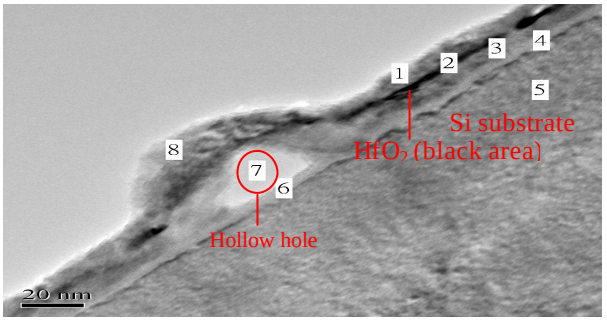

Fig.3 TEM micrograph of $TiN/Al_2O_3/HfO_2/Al_2O_3/TiN/SiO_2/Si$ sample after 1000°C RTA in N_2.

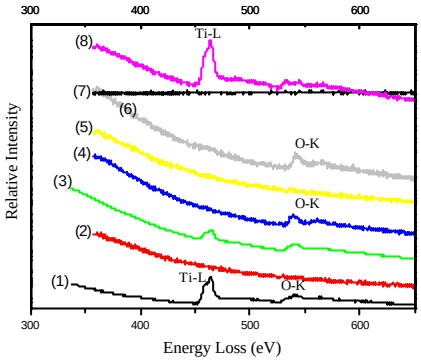

Fig. 4 EELS spectra at various locations which are identified in Fig. 3.

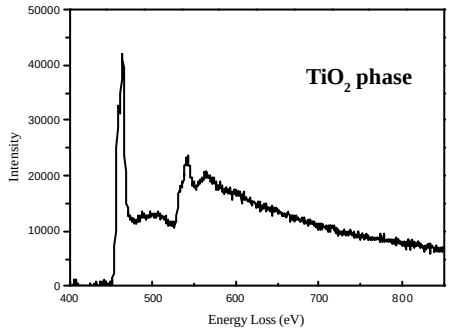

Fig. 5 EELS Ti-O bonding signal extracted from the curve (1) of Fig. 4.

To further study the N content in the TiN film, EDS was employed. Figure 6(A) shows the original TEM micrograph of the raised-hollow hole in the annealed sample and Figure 6(B) depicts the EDS nitrogen mapping image of Fig. 6(A). None of nitrogen content can be seen from the Fig. 6(B). This evidenced that the nitrogen was desorbed from TiN during the high temperature annealing.

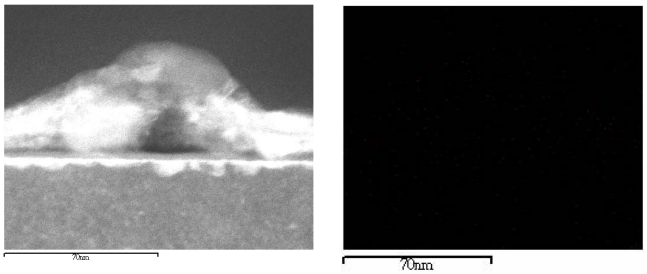

(A) (B)

Fig. 6 EDS mapping image, (A) original image; (B) nitrogen mapping image.

Figure 7 shows the HR-TEM micrographs of samples before and after RTA. For the as-deposited one, the interface between each layer is distinct, however, the Al_2O_3/TiN interface was disappeared after RTA. On the other hand, very obvious morie fringes can be seen through the whole Al_2O_3/TiO_2 mixed layer in the 1000°C annealed sample. Also, the HfO_2 had crystallized.

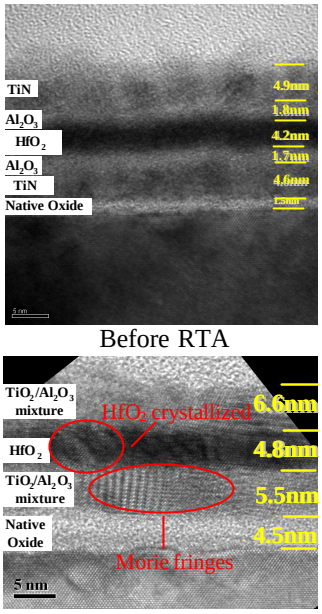

Fig. 7 HR-TEM micrographs of MIM samples before and after RTA.

At the high temperature (1000°C), the TiN would mix with the Al_2O_3 and the oxygen content in the Al_2O_3 might further oxidize the TiN film. The desorption of nitrogen in TiN film might result from the oxidation of TiN. Also, the hollow hole, as seen from Fig. 3, would result from the intrinsic stress in the films were enhanced during the oxidation of TiN. The TiN film is easily oxidized since the oxygen can diffuse through the grain boundary of TiN grain [4]. The diffusion of oxygen can result in the oxidation of the whole TiN film in addition to the surface.

4. Conclusion

The microstructure of TiN/Al_2O_3/HfO_2/Al_2O_3/TiN /SiO_2/Si MIM capacitor prepared by ALD system at elevated temperature was studied. Experimental results indicated that the high temperature can result in the inter-diffusion of Al_2O_3 and TiN films and very clear morie fringes can be seen from the TEM micrographs. Also, the nitrogen content in TiN was desorbed. This phenomenon might result from the oxidization of the TiN film where the oxygen might contribute from the Al_2O_3 layer.

References

[1] The International Technology Roadmap For Semiconductors, (2004) 32.

[2] Y. H. Lin, C. H. Chien, C. T. Lin, C. Y. Chang, and T. F. Lei, IEEE Elec. Devi. Lett. **26** (2005) 154.

[3] K. E. Elers, V. Saanila, P. J. Soininen, W. M. Li, J. T. Kostamo, S. Hankka, J. Juhanoja, W. F. A. Besling, Chem. Vapo. Depos. **8** (2002) 149.

[4] S. Logothetidis, E. I. Meletis G. Stergioudis, A. A. Adjaottor Thin Solid Films **338** (1999) 304.